Asian Journal of Information Technology 15 (17): 3134-3152, 2016
ISSN: 1682-3915

Performance Study of Kriging Based Surrogate Models

[1]A. Muruganandham, [2]R. Mukesh, [3]K. Lingadurai and [4]U. Selvakumar
[1]Department of ECE, Shree Sathyam College of Engineering and Technology, Sankari, Tamil Nadu, India
[2]Department of Aeronautical Engineering, ACS College of Engineering, Bangalore, India
[3]Department of Mechanical Engineering, Anna University, Dindigul, India
[4]Department of Information Technology, Ghent University, Belgium, Ghent, India

Abstract: The use of optimisers in the Kriging based surrogate models has become popular in full-scale aerospace systems development. Computational modelling through high-fidelity simulations provides a possible approach towards efficient implementation of the design specifications but the associated computational cost restricts its applicability to full-scaled systems. In this present research a Computational Fluid Dynamics (CFD) optimisation strategy based on surrogate modelling is proposed for obtaining high-fidelity predictions of aerodynamic forces (Cl, Cd) and aerodynamic Efficiency (E). An Aerodynamic Shape Optimisation (ASO) problem is formulated and solved using Particle Swarm Optimisation Algorithm (PSOA) and Modified Particle Swarm Optimisation Algorithm (MPSOA) with the inclusion of constructed surrogate models in the place of actual CFD algorithms. Ordinary Kriging (OK) approach is used to construct the surrogate models. PARametric SECtion (PARSEC) approach is implemented to mathematically describe the geometry of the airfoil. The results of two optimisers and an airfoil shape optimisation problem shows that this approach, known as MPSOA can significantly enhance the accuracy of Kriging models when compared to the normal PSOA.

Key words: Surrogate model, OK, PSOA, MPSOA, aerodynamic efficiency

INTRODUCTION

The computational cost involved in performing numerical simulations for designing and optimising various engineering systems such as aircraft wings, is continuously increasing. From an engineering perspective, the design process is crucial for achieving maximum efficiency with the minimum possible cost and within the manufacturing restrictions. In the context of aircraft wings, ASO techniques are of great importance for designing a lifting surface with maximum aerodynamic efficiency. In ASO, aerodynamic constraints such as flow properties, Mach number (M), etc. alone are taken into account in contrast to Multidisciplinary Design Optimisation (MDO) where constraints from various disciplines such as financial, structural, manufacturing, etc. are considered. The constraints of the optimisation problem define the spectrum of the design variables and strongly influence the search space where the optimal solution lies. Parameterisation parameters, which will parameterise the geometry of the engineering system to be optimised, serve as a part of the design variables of the optimisation problem. The range of values of the design variables is defined, subject to the satisfaction of optimisation problem constraints. Since the number of design variables directly influences the complexity of the problem, various parameterisation approaches such as Discrete point approach, Partial differential equation approach and Polynomial approach have been developed with the intention of simplifying the parameter space without compromising the accurate description of the geometry (Balu and Selvakumar, 2009). PARSEC which is employed in the current work, is one of the parametric polynomial geometry representation approaches.

In this research both the high and low fidelity solvers are used to solve the flow governing equations. Here, the high-and low-fidelity solvers refer the numerical solution of the governing equations through CFD simulation software (ANSYS Fluent) and the use of Panel method respectively. The optimisation schemes can be broadly classified into two different categories: Gradient-based or Derivative optimisation schemes and Non-Derivative or Evolutionary optimisation schemes. When the traditional gradient-based optimisation schemes are employed for their exploitation property, the choice of the starting point becomes increasingly important, as the gradient-based schemes are more likely to be converged or stuck into local optima (Zang and Green, 1999; Raymer, 2002). On the other hand, the non-derivative methods are

Corresponding Author: A. Muruganandham Department of ECE, Shree Sathyam College of Engineering and Technology, Sankari, Tamil Nadu India

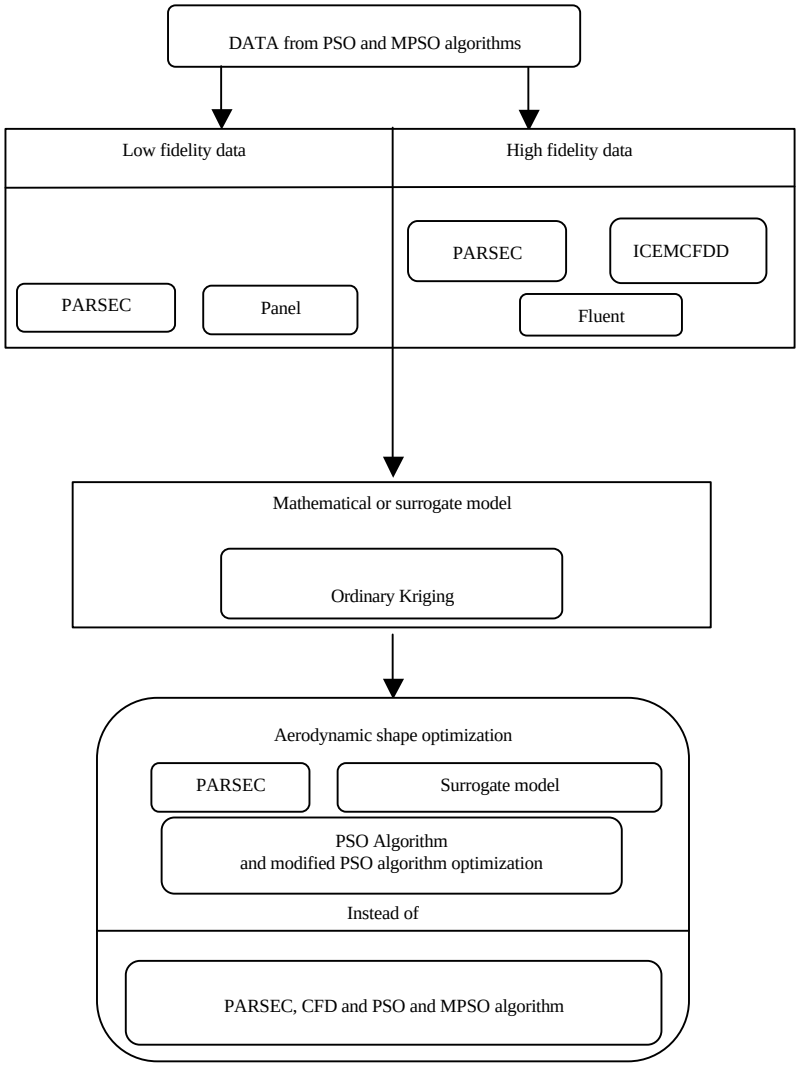

Fig. 1: Processes involved with the proposed approach

more powerful in finding the global optimum within the given search space, to that end we have employed both the PSO and MPSO algorithms in this research.

ASO problem is formulated in this work to identify the best possible airfoil geometry which will have an improved E for the given flow, structural and aerodynamic conditions. The problem considers the NACA 2411 geometry as a base line shape and is solved using PSOA and MPSOA. The flow is viscous, compressible and low turbulent, with M varying between 0.1 and 0.6 with fixed angle of attack of 5.0. The aerodynamic constraint of the problem is that the E of the optimised airfoil should not be less than that of the base line airfoil. The structural constraints of the problem are that the trailing edge thickness (T_{te}) and trailing edge offset (T_{off}) of the airfoil should be zero. In this research, PARSEC approach is employed to mathematically describe the geometry of the airfoil due its robustness and flexibility in controlling the aerodynamic characteristics with less number of parameters. OK approach is employed to construct surrogate models due to its statistically unbiased optimal prediction capability (Giunta, 1997). Figure 1 depicts the work flow of the proposed ASO strategy.

PARSEC: The lower and upper surfaces of an airfoil are described independently using a sixth order polynomial method called PARSEC parameterisation scheme (Sobieczky, 1998). In this approach, the shape of the airfoil is controlled by the twelve parameters (Castonguay and Nadarajah, 2007; Ulaganathan *et al*., 2010) which are listed in Table 1 and also shown in Fig. 2.

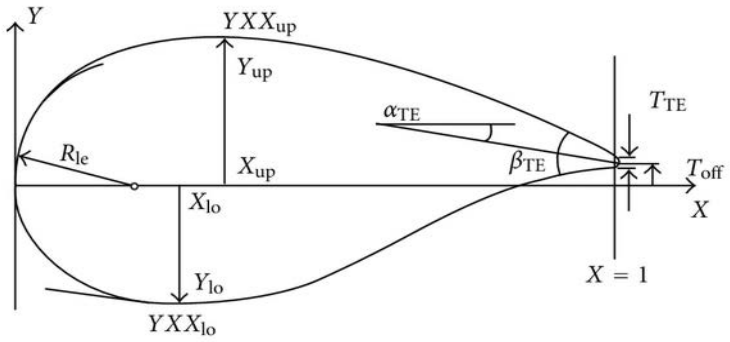

Fig. 2: Control parameters of PARSEC

Table 1: Design variables and their range of values

Design parameters	Range values for NACA 2411 Airfoil: Lower bound values	Upper bound values
(Rleu) Upper leading edge radius	0.020	0.023
(Rlel) Lower leading edge radius	0.006	0.010
(Xup) Position of upper crest	0.320	0.370
(Yup) Upper crest point	0.077	0.080
(YXXup) Upper crest curvature	-0.630	-0.650
(Xlo) Position of lower crest	0.150	0.190
(Ylo) Lower crest point	-0.020	-0.050
(YXXlo) Lower crest curvature	0.600	0.750
(áTE) Trailing edge direction angle	-4.550	-4.900
(âTE) Trailing edge wedge angle	15.000	15.100

The mathematical formulation of the approach is given by Eq. 1 and 2 for the upper and lower surfaces of the airfoil, respectively:

$$y_u = \sum_{i=1}^{6} a_i x^{i-(1/2)} \quad (1)$$

$$y_l = \sum_{i=1}^{6} b_i x^{i-(1/2)} \quad (2)$$

Where:

y_u = The y co-ordinate for the upper surface
y_l = The y co-ordinate for the lower surface,
x = The non-dimensional chord-wise location (chord (c) is assumed to be 1)
a_i and b_i = The coefficients to be solved

The surface of the airfoil is obtained from the solution of the above two equations subject to the geometrical conditions:

- At x = maximum, y = maximum
- At x = maximum $\frac{dy}{dx} = 0$
- At x = maximum, $\frac{d^2y}{dx^2}$ = maximum
- At xup = 1, $y_{up} = T_{off} + \frac{T_{TE}}{2}$
- At x_{lo} = 1, $y_{lo} = T_{off} - \frac{T_{TE}}{2}$
- At $x_{lo} = 1 \frac{dy_{up}}{dx} = \tan\left(\alpha_{TE} - \frac{\beta_{TE}}{2}\right)$
- At $X_{lo} = 1, \frac{dy_{lo}}{dx} = \tan\left(\alpha_{TE} + \frac{\beta_{TE}}{2}\right)$

Ordinary Kriging (OK): Kriging which was proposed by Sacks *et al.* (1989) for the design and analysis of computer experiments is very popular in Computer Aided Engineering (CAE) applications. For interpolations of random responses the Kriging techniques are employed Stein (1999). The mathematical expression for the function to be defined is given by Eq. 3 during the usage of ordinary Kriging approach (Duchaine *et al.*, 2009; Jouhaud *et al.*, 2007):

$$\hat{f}(x_p) = \sum_{i=1}^{N} \gamma_i(x_p) f(x_i) \quad \forall x_p \in S \quad (3)$$

Where :

$\hat{f}$ = The function of linear estimation for
$f, \gamma_i(x_p)$ = The weighting function and
x_p = A vector of sample points in the design space

which in our case is defined through the range of values of 10 PARSEC parameters along with the M and is denoted by $S \subset R^{11}$. The covariance of f between two sample points is described by a function which is based on the distance between the two sample points and it is given in Eq. 4:

$$C[f(x_a), f(x_b)] = C[|x_a - x_b|] \quad (4)$$

C [$f(x_a)$, $f(x_b)$] is often expressed by the covariance matrix as given:

$$\underline{C} = \begin{pmatrix} \sigma^2 = C(0) & C(\|x_1 - x_2\|) & \cdots & C(\|x_1 - x_N\|) \\ C(\|x_2 - x_1\|) & \sigma^2 & \cdots & C(\|x_2 - x_N\|) \\ \vdots & \vdots & \vdots & \vdots \\ C(\|x_N - x_1\|) & C(\|x_N - x_2\|) & \cdots & \sigma^2 \end{pmatrix} \tag{5}$$

The variance of the sample points is given as σ^2. The covariance vecto $(\vec{c})$ r and the weighting functions vector can be expressed as follows for the unknown sample point $x_p \in S$:

$$\vec{c}(x_p) = \begin{pmatrix} C(\|x_p - x_1\|) \\ C(\|x_p - x_2\|) \\ \vdots \\ C(\|x_p - x_N\|) \end{pmatrix}; \gamma_i(x_p) = \begin{pmatrix} \gamma_1(x_p) \\ \gamma_2(x_p) \\ \vdots \\ \gamma_N(x_p) \end{pmatrix} \tag{6}$$

For an isotropic stationary model, the sum of all the weighting functions should be equal to unity as given in Eq. 7. Hence, the covariance matrix and covariance vector become as given in Eq 8 and 9, respectively:

$$\sum_{i=1}^{N} \gamma_i(x_p) = 1 \quad \forall x_p \in S \tag{7}$$

$$\underline{C} = \begin{pmatrix} \sigma^2 = C(0) & C(\|x_1 - x_2\|) & \cdots & C(\|x_1 - x_N\|) & 1 \\ C(\|x_2 - x_1\|) & \sigma^2 & \cdots & C(\|x_2 - x_N\|) & 1 \\ \vdots & \vdots & \ddots & \vdots & \vdots \\ C(\|x_N - x_1\|) & C(\|x_N - x_2\|) & \cdots & \sigma^2 & 1 \\ 1 & 1 & \cdots & 1 & 0 \end{pmatrix} \tag{8}$$

$$\vec{c}(x_p) = \begin{pmatrix} C(\|x_p - x_1\|) \\ C(\|x_p - x_2\|) \\ \vdots \\ C(\|x_p - x_N\|) \\ 1 \end{pmatrix} \tag{9}$$

A Lagrange multiplier (λx_p) is introduced in the weighting functions vector in order to enforce the unbiasedness constraint of the OK model. Hence, the weighting functions vector becomes as follows:

$$\gamma_i(x_p) = \begin{pmatrix} \gamma_1(x_p) \\ \gamma_2(x_p) \\ \vdots \\ \gamma_N(x_p) \\ \lambda_{x_p} \end{pmatrix} \tag{10}$$

The weighting functions are calculated using the covariance matrix and covariance vector as given by the following relation:

$$\gamma(x_p) = \underline{C}^{-1}\vec{c}(x_p) \tag{11}$$

Since, the predicted value of the response is always different from the actual value at the sample point, an error measure is introduced to measure the prediction capability of the OK model. This measure of error is known as estimation error (e_p) and is defined as follows:

$$e_p = \hat{f}(x_p) - f(x_p) \tag{12}$$

where, $f(x_p)$ is the actual value at an unknown point $x_p \in S$. If the weighting functions are obtained in such a way that they will reduce the variance of the estimation error, then a function predictor with optimal prediction capability can be obtained. The error variance can be computed using the following expression:

$$V(e_p) = \sum_{i=1}^{N} (\vec{c}(x_p)\gamma_i(x_p)) \tag{13}$$

Since, the covariogram function is arbitrarily computed from the observed data, a suitable theoretical variogram model should be used to fit the experimental variogram model, so that the Kriging equations become solvable. Generally, the selection of a suitable theoretical variogram model is carried out using Maximum Likelihood Estimation (MLE) or Cross Validation (CV) approaches. In the current work, the following theoretical variogram models are employed and the most suitable one is selected based on the CV approach (Rodriguez *et al*., 2010; Balu *et al*., 2012).

Gaussian model with actual range:

$$C(h) = sill\left(1 - \exp\left(\frac{-h^2}{r^2}\right)\right) \tag{14}$$

Gaussian model with practical range:

$$C(h) = sill\left(1 - \exp\left(\frac{-3h^2}{pr^2}\right)\right) \tag{15}$$

Spherical model with actual range:

$$C(h) = sill\left(\left(\frac{3.0}{2.0}\right)\left(\frac{h}{range}\right) - 0.5\left(\frac{h}{range}\right)^3\right) \tag{16}$$

Exponential model with actual range:

$$C(h) = sill\left(1 - \exp\left(\frac{-h}{range}\right)\right) \quad (17)$$

Exponential model with practical range:

$$C(h) = sill\left(1 - \exp\left(\frac{-3h}{prange}\right)\right) \quad (18)$$

where, h is the isotropic lag defined as the distance between two sample points in S. In the semivariogram, the lag value at which the semivariance becomes constant is called as range and the corresponding semivariance value is called as sill. The practical range is the value of lag at which 0.94% of the sill is achieved.

PSO algorithm: PSO was originally developed by James Kennedy and Russell Eberhart in the year of 1995 to simulate the motion of swarm of birds as part of a Socio-cognitive study. It is a population based optimisation technique which searches for the global optimum (Ping and Jiang, 2008; Yang *et al*., 2011; Liang *et al*., 2011). It's a simple and powerful search technique. PSO algorithm is not only a tool for optimisation but also a tool for representing socio-cognition of human and artificial agents, based on principles of social psychology. A PSO system combines local search methods with global search methods, attempting to balance exploration and exploitation. In PSO, a swarm of 'n' individuals communicate either directly or indirectly with one another search directions. Each individual is called as a particle which is searching for the optimum. Each particle is moving and hence has a velocity. Each particle remembers the position it was in where it had its best result so far and this value is called as pbest or its personal best. Another best value obtained so far by any particle in the neighbourhood when compared to all the particles in the domain is called as gbest or global best. The Algorithm for the PSO technique is given below by assuming N particles in the swarm in the D dimensional search space. Here the ith particle is represented as: $X_i = (x_{i1}, x_{i2}, ...x_{id})$. The best precious position giving the best fitness value is represented as $P_i = (p_{i1}, p_{i2} ...p_{id})$ and the rate of change (velocity) of the particle is given as $V_i = (v_{i1}, v_{i2},...v_{id})$. The velocity and position are updated by the following equations:

$$v_{i,d}(t) = v_{i,d}(t-1) + c_1.\phi_1.(p^{*}_{i,d} - p_{i,d}(t-1)) + c_2.\phi_2.(p^{\#}_{d} - p_{i,d}(t-1)) \quad (19)$$

Table 2: The MPSO parameters to control the evolution (ASO)

Parameters	Values
No. of particles	24
No. of generations	100
ω	0.5
Velocity	Unrestricted velocity
C_{1g}, C_{1b} and C_2	0.6
ϕ1-3	0.7
Angle of attack	5.0 deg
Geometric constraint	Max thickness must be <10% chord length Min thickness must be >1% chord length and the airfoil is zero
Objective	Maximum aerodynamic efficiency
Termination condition	Terminate when there is a change of $<10^{-5}$ in the successive values of the best fitness function value (Cl)

$$p_{i,d}(t) = p_{i,d}(t-1) + v_{i,d}(t) \quad (20)$$

In the above equations the $p_{i,d}$ indicates the best position of ith particle up to time t-1 which is denoted as P_{best} and $p^{\#}_{d}$ indicates the best position of the whole swarm up to time t-1 which is denoted as G_{best}. The random numbers are denoted as φ_1 and φ_2 furthermore the c_1 represents the individuality coefficients and c_2 represents sociality coefficients. In the current problem we have initially determined the population size and then we have fixed the value for the coefficients c_1 and c_2 which are tabulated in Table 2. Subsequently, the position and velocity (unrestricted velocity) of each particle are initialized. According to Eq. 19 and 20 each particle moves in the search domain and the fitness is calculated. At the same time, the best positions of each particle and the swarm are recorded. Finally, the stopping criterion is achieved; the best position of the swarm is the final solution (Khurana *et al*., 2009; Mukesh *et al*., 2012, 2014).

Modified PSO: In this modified PSO the cognitive component of the normal PSO is divided into two components. The first component is called as good experience component which means that the particle has a memory about its previously visited best position. The second component is called as bad experience component which means that the particle has a memory about its previously visited worst position (Deepa and Sugumaran, 2011). To calculate the new velocity, the bad experience is also considered and by using that component, the particle can bypass its previous worst position and try to find the better position (Deepa and Sugumaran, 2012; Qin *et al*., 2009). The searching behaviour of the modified PSO algorithm is shown in Fig. 3 and flow chart of the modified PSO is given in Fig. 4. The modified velocity update equation is given by:

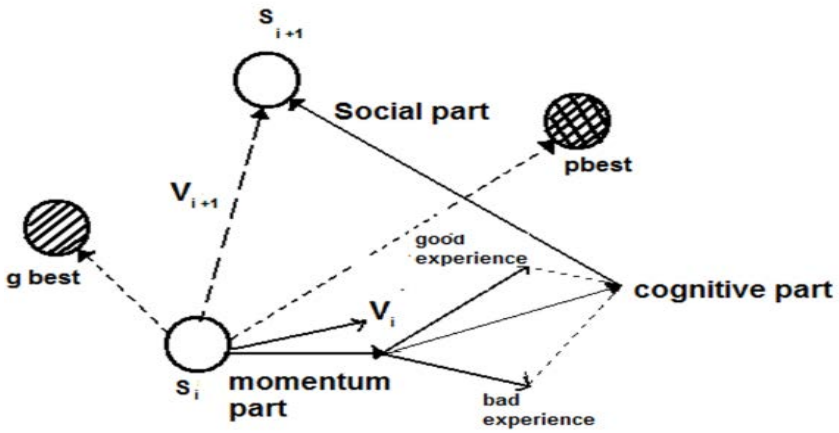

Fig. 3: Searching behaviour of MPSO

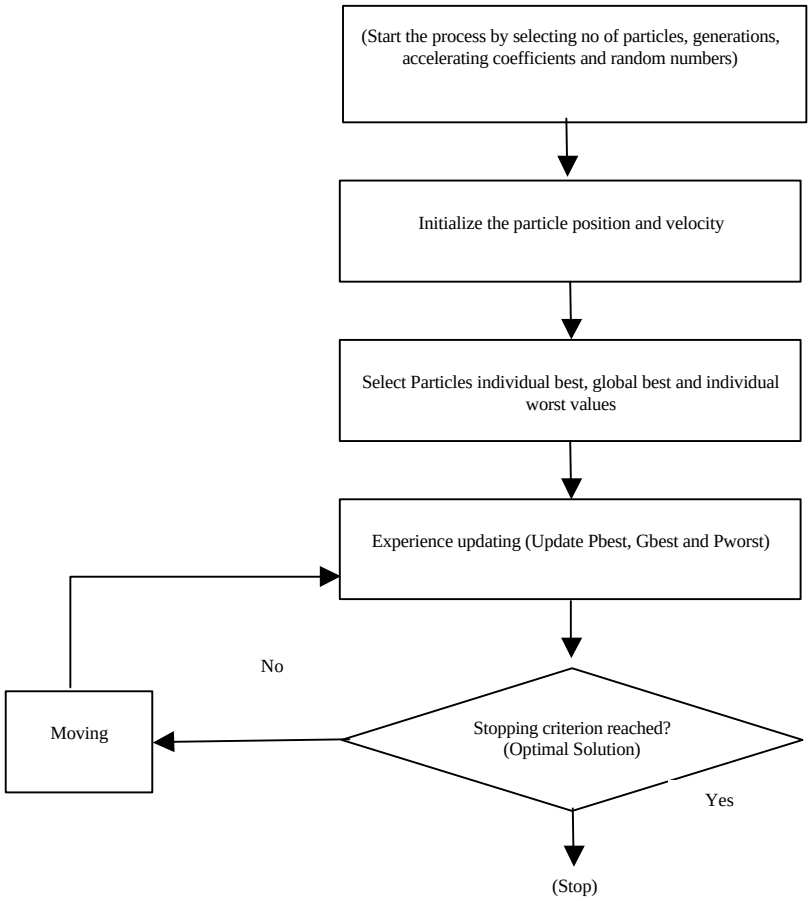

Fig. 4: Flow chart of MPSO

$$V_{i+1} = \omega x V_i + C_{1g} x \varphi 1 x \left(P_{best\,i} - S_i\right) + C_{1b} x \varphi 2 x \left(S_i - P_{worst\,i}\right) + C_2 x \varphi 3 x \left(g_{best\,i} - S_i\right) \quad (21)$$

Where:

C_{1g} = Acceleration coefficient, accelerates the particle towards its best position

C_{1b} = Acceleration coefficient, accelerates the particle away from its worst position
C_2 = Social acceleration coefficient
P_{besti} = Personal best position of the ith particle
$P_{worst\ I}$ = Worst position of the ith particle
$g_{best\ I}$ = Global best position of the ith particle
ω = Inertia weight
$\varphi 1\text{-}3$ = Random numbers

RESULTS AND DISCUSSION

The optimal sample points are generated by the PSO and MPSO algorithm and in order to get the data, computer-based simulations are needed to be performed at the generated sample points. During the construction of surrogate models those collected datas are used to initiate the learning process (Mukesh *et al*., 2014). As mentioned earlier, the dimension (n) and the design space of the current problem are 11 and $S \subset R^{11}$, respectively. Table 1 gives the design variables and their range of values for the current problem. A sample point has 10 PARSEC parameters and a M. About 50 (N) such sample points are randomly taken from the optimizers generated sample points where the simulations are needed to be performed.

Computer-based simulations, both panel (low-fidelity) and CFD (high-fidelity) have been performed at these 50 sample points. A Linear Vorticity Surface Panel method code developed by Ilan Kroo is used for the low-fidelity simulations. Panel methods are more effective in giving reasonably accurate results without being computationally expensive. The flow around the NACA 2411 airfoil is solved using the panel code for 5 deg angle of attack with Np = 1000 (Number of panels). High fidelity, CFD simulations are performed by solving two-dimensional, steady and compressible Navier-Stokes equations using FLUENT software.

Low fidelity solver: The solution Panel method which gives more accurate results is used to solve the potential equations. This approach is employed in this work to deal with the incompressible flow. The solution procedure for panel technique consists of discretizing the surface of the airfoil by assuming the source strength is constant over each panel but has a different value for each panel and the vortex strength is constant and equal over each panel (Hess, 1990; Katz and Plotkin, 1991). The curl of the velocity field is assumed to be zero. Figure 5 illustrates the nodes and panels for panel methods respectively. The coefficient of pressure can be found by using Eq. 22:

$$c_p(x_i, y_i) = 1 - [V_{ti}^2 / V_{CQ}^2] \quad (22)$$

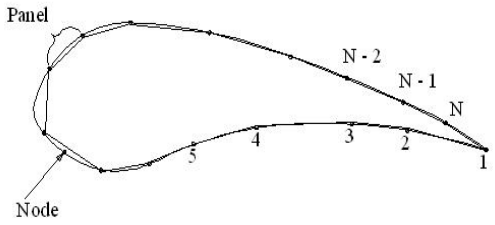

Fig. 5: Nodes and panels

High fidelity solver: High fidelity, CFD simulations are performed by using FLUENT Software. The turbulence phenomena have been modelled through the Spalart-Allmaras turbulence model which is a one-equation model solving the turbulent viscosity transport equation (Spalart and Allmaras, 1992; Wilcox, 1993) and has been widely used for aerospace applications. The computational grid is generated with ICEM CFD package. C-grid topology is used since it is quite good in capturing the flow physics in the wake region of the airfoil (Zang and Green, 1998). In order to capture the flow physics within the boundary layer region, $y^+ = 1$ has been used (2011).

Density-based implicit solver in FLUENT is used to solve the flow around the airfoil geometry with ideal gas as a working fluid. The viscosity is calculated from the co-efficient Sutherland law and the turbulence is specified in terms of turbulent intensity (I) and turbulent length scale (l) and Least Squares Cell Based discretisation scheme is used for gradient together with the Roe-FDS flux type. Third order Monotone Upstream-centred Schemes for Conservation Laws (MUSCL), which can provide more accurate numerical results even when the solutions exhibit shock, are employed for the spatial discretisation of the flow (Alexander and Tadmor, 2010; Konstantin and Metodiev; Sheldahl and Klimas, 1981).

In order to validate the mesh generation and solution techniques, flow over the NACA 2411 airfoil is solved using the above described mesh generation and solution methods. The grid generation process for the remaining 50 sample points is automated so that the same grid generation technique can be applied for all the airfoil geometries. It is also ensured that the applied grid generation technique results to a fine mesh for all the airfoil geometries. The flow around the 50 airfoil geometries is solved using both the low-fidelity panel simulations and high-fidelity CFD simulations. Once the aerodynamic forces ((Cl) Low-fidelity, (Cl) High-fidelity and (Cd) High- fidelity) are obtained for the generated 50 airfoil geometries, then they can be used for the learning process.

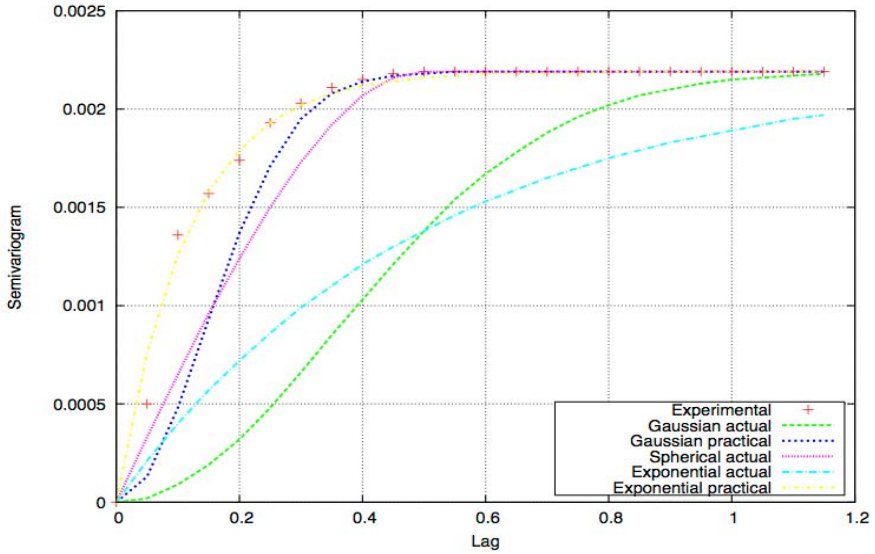

Fig. 6: Theoretical semivariogram models (low-fidelity Cl) based on PSOA

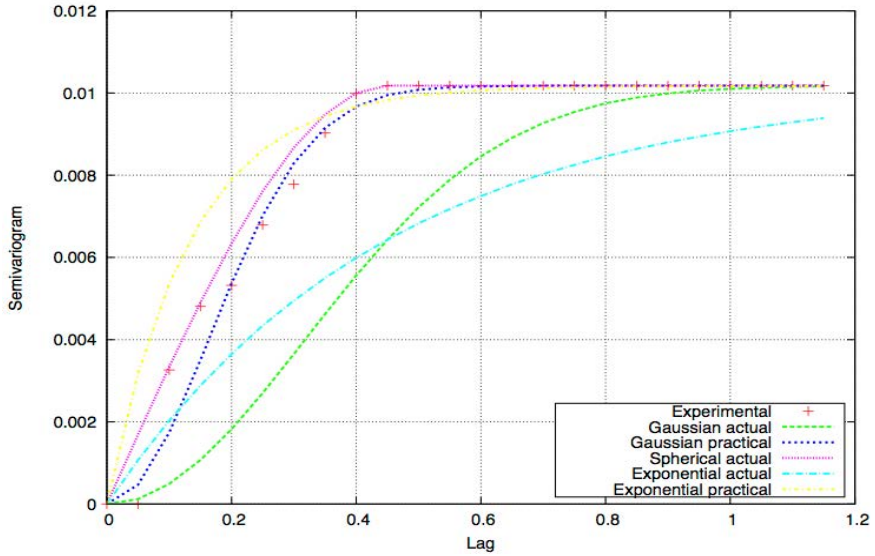

Fig. 7: Theoretical semivariogram models (low-fidelity Cl) based on MPSOA

Three surrogate models are constructed using the in-house OK code. The first surrogate model is constructed using the low-fidelity panel data and can predict the low-fidelity Cl for any airfoil geometry placed within the design space S. The second surrogate model is constructed using the high-fidelity C_d data and can predict the high-fidelity C_d for any airfoil geometry placed within S. The third one is constructed using the difference in Cl between the low- and high-fidelity data (ΔCl) and can be used to estimate the difference in Cl between the low-and high fidelity analysis for any airfoil geometry placed within S .

Figure 6-11 shows the capability of different theoretical semivariogram models in fitting the experimental semivariogram model for the first, second and third surrogate models, respectively which have been generated based on the data obtained from PSO and MPSO algorithms. It can be clearly observed that the Exponential model with practical range is fitting the experimental semivariogram model more accurately than any other theoretical models for all the three surrogate models. The second most accurate one is the Gaussian model with practical range.

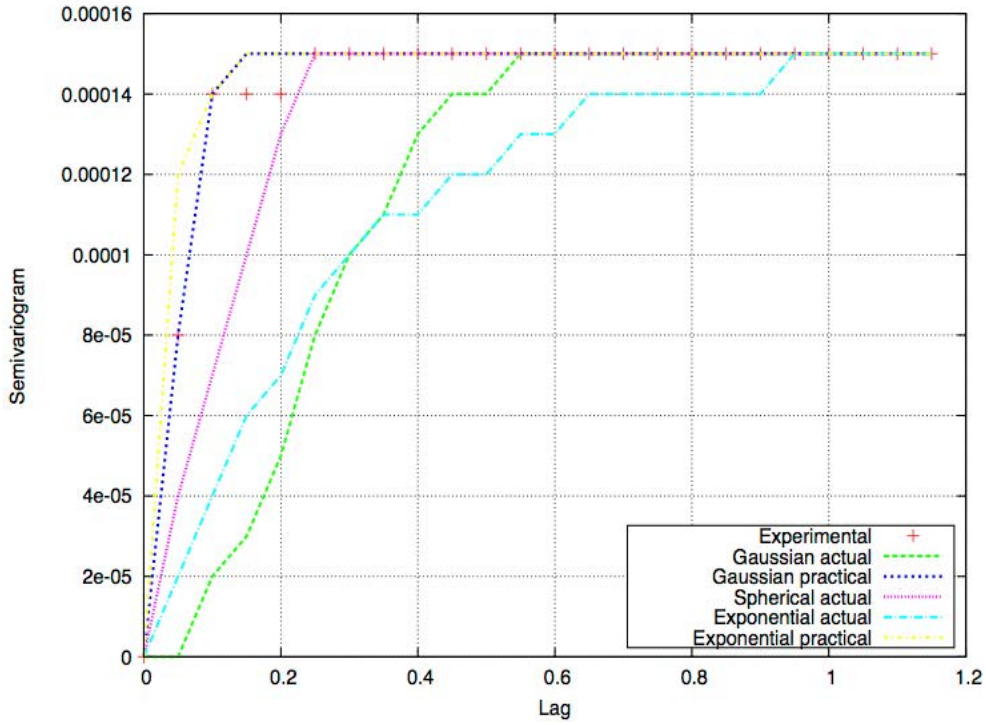

Fig. 8: Theoretical semivariogram models (High-fidelity Cd) based on PSOA

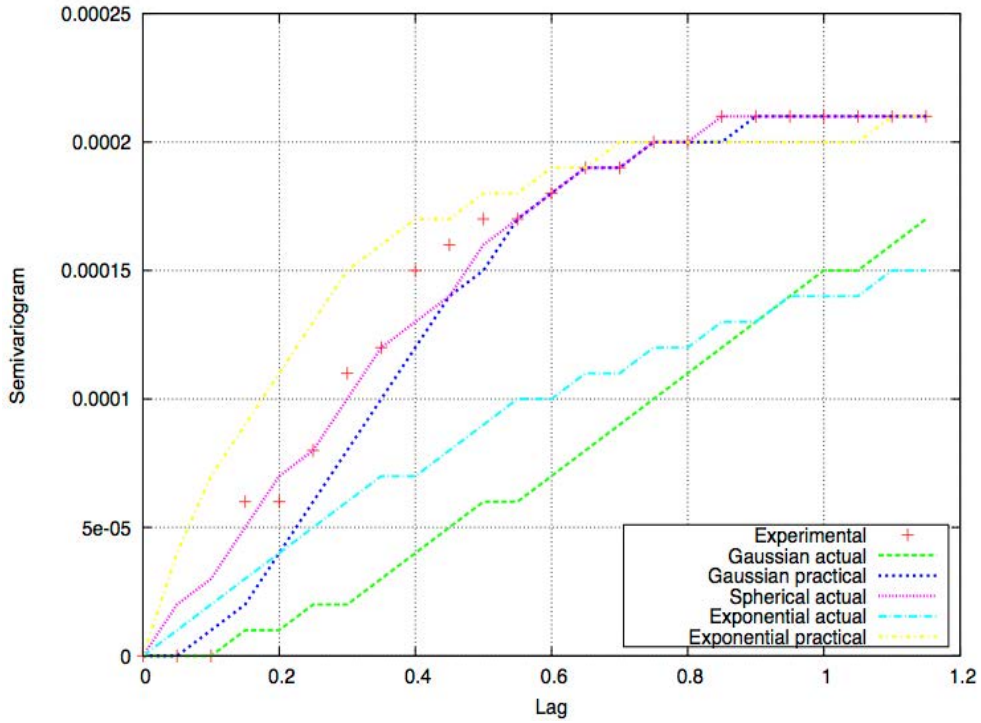

Fig. 9: Theoretical semivariogram models (High-fidelity Cd) based on MPSOA

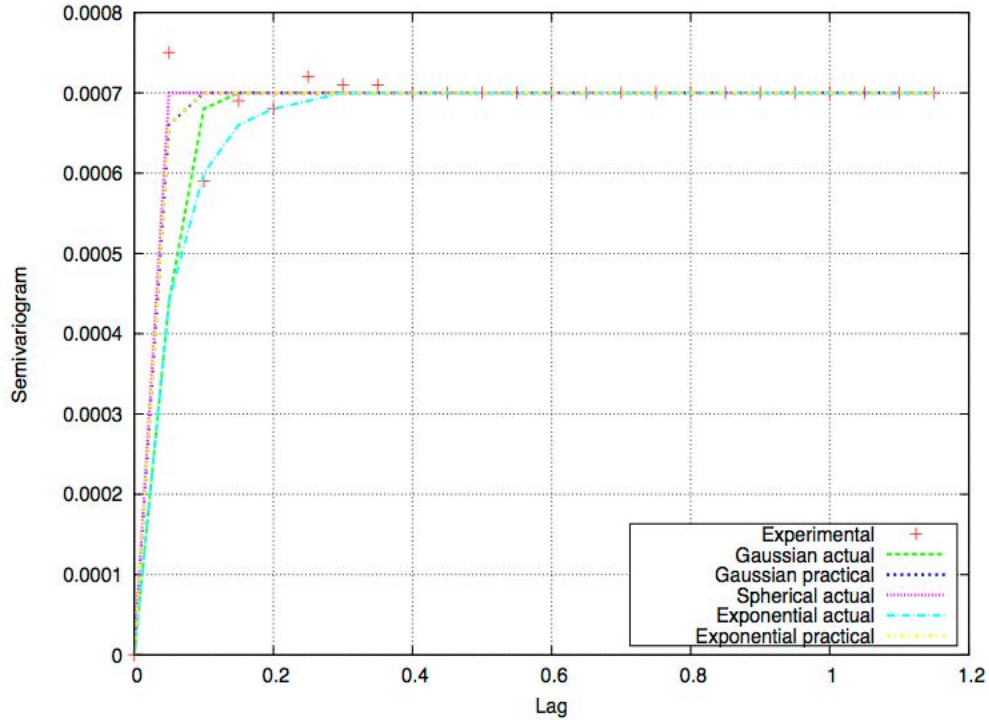

Fig. 10: Theoretical semivariogram models (ΔCl) based on PSOA

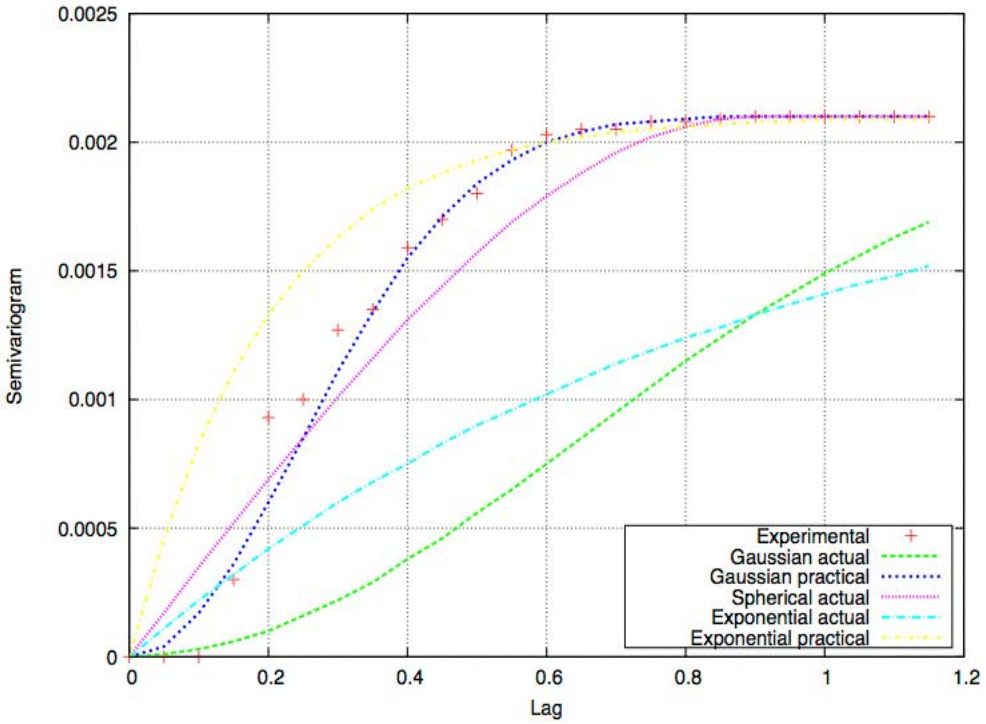

Fig. 11: Theoretical semivariogram models (ΔCl) based on MPSOA

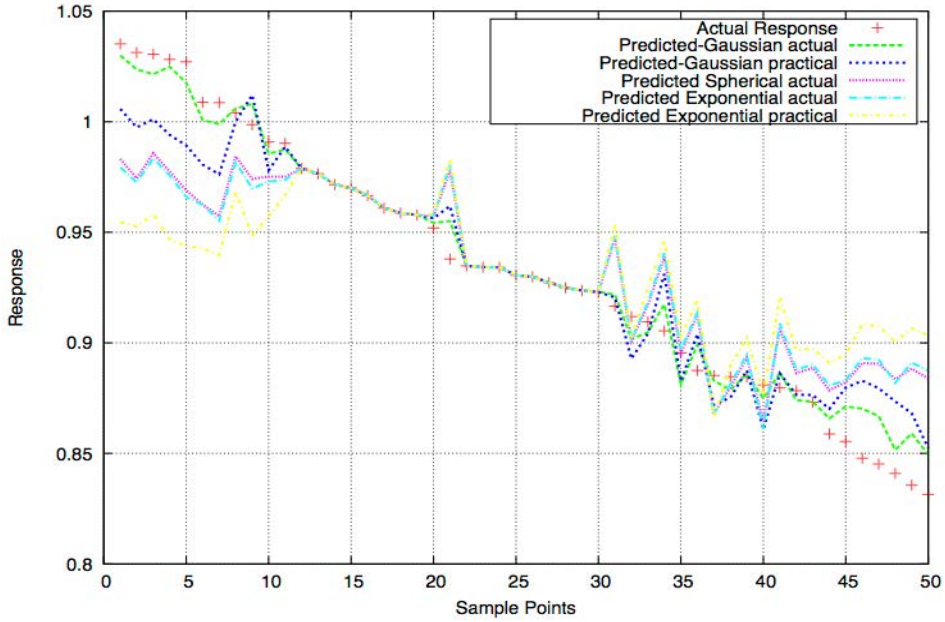

Fig. 12: Sample points and its responses (Low-fidelity Cl) based on PSOA

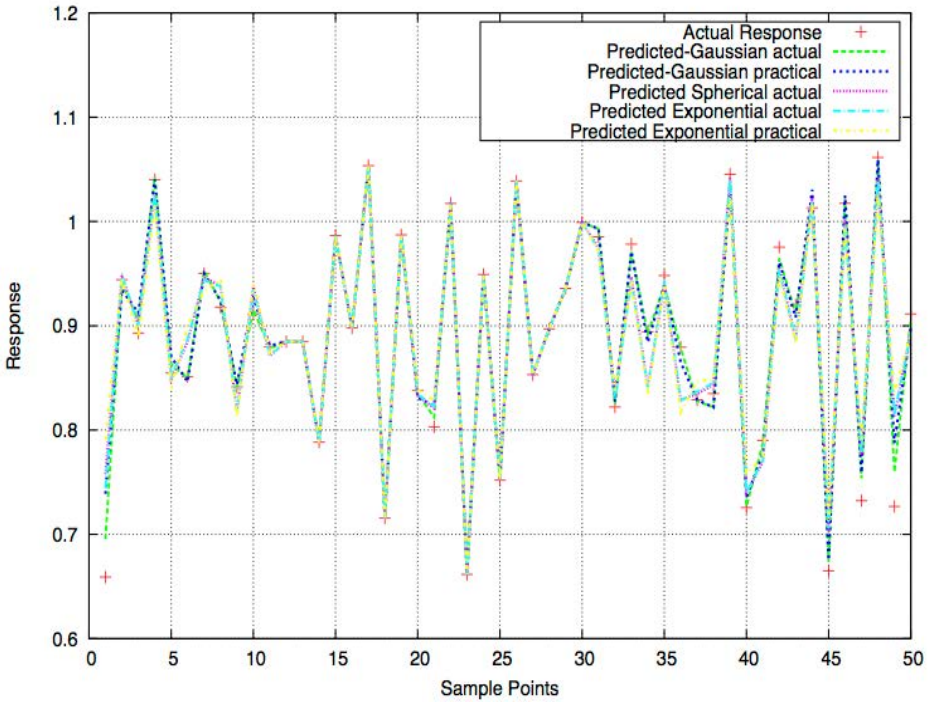

Fig. 13: Sample Points and its responses (Low-fidelity Cl) based on MPSOA

Figures 12-17 shows the sample points and its response for the datas generated by the PSO and MPSO algorithms. It can be observed that the Exponential model with practical range and the Gaussian model with practical range are fitting to the actual response than any other theoretical models.

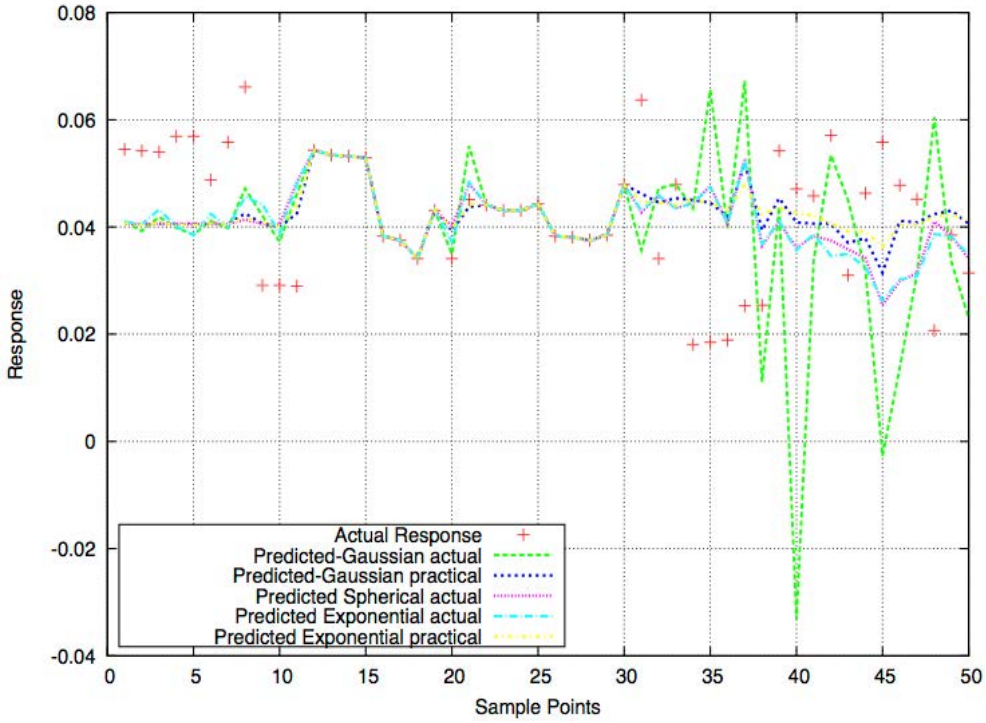

Fig. 14: Sample points and its responses (High-fidelity Cd) based on PSOA

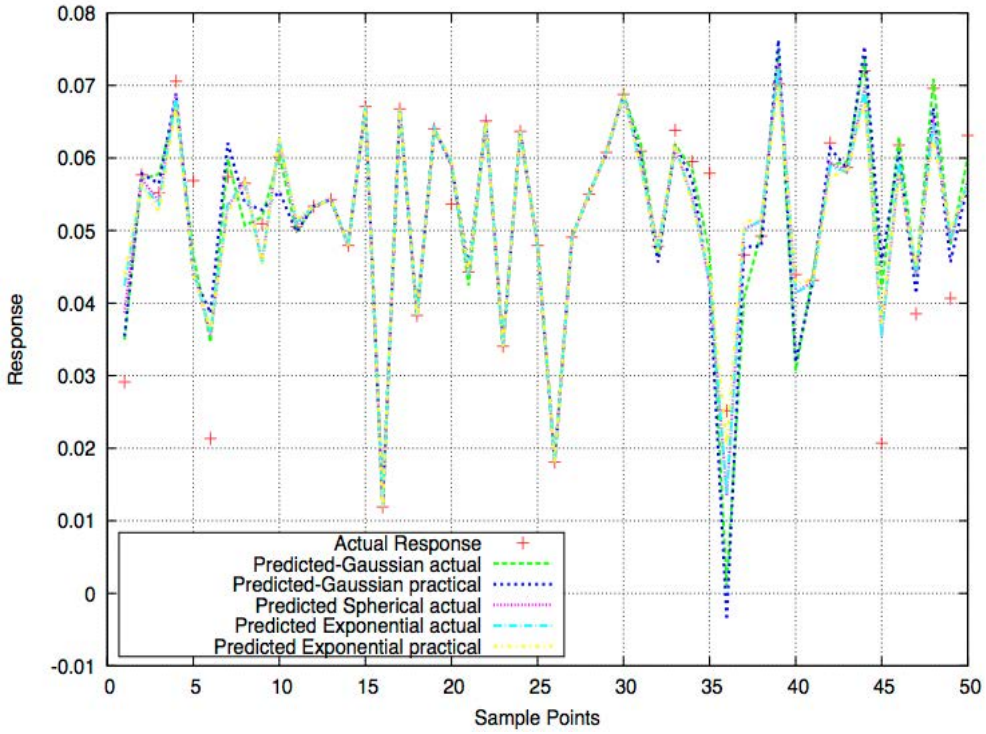

Fig. 15: Sample points and its responses (High-fidelity Cd) based on MPSOA

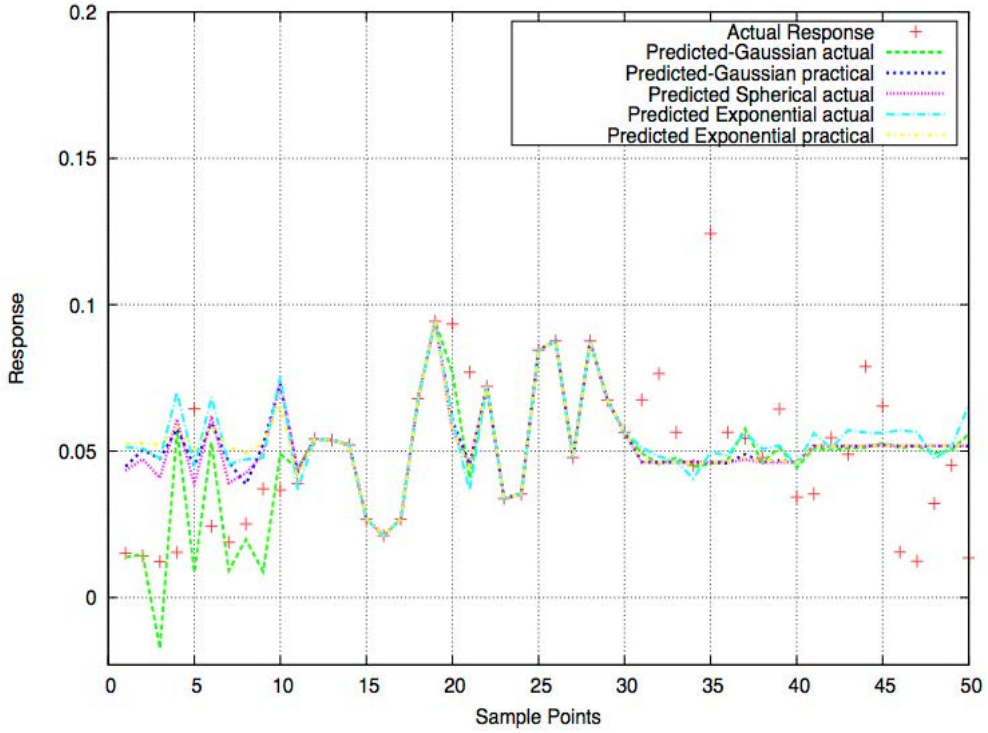

Fig. 16: Sample points and its responses (ΔCl) based on PSOA

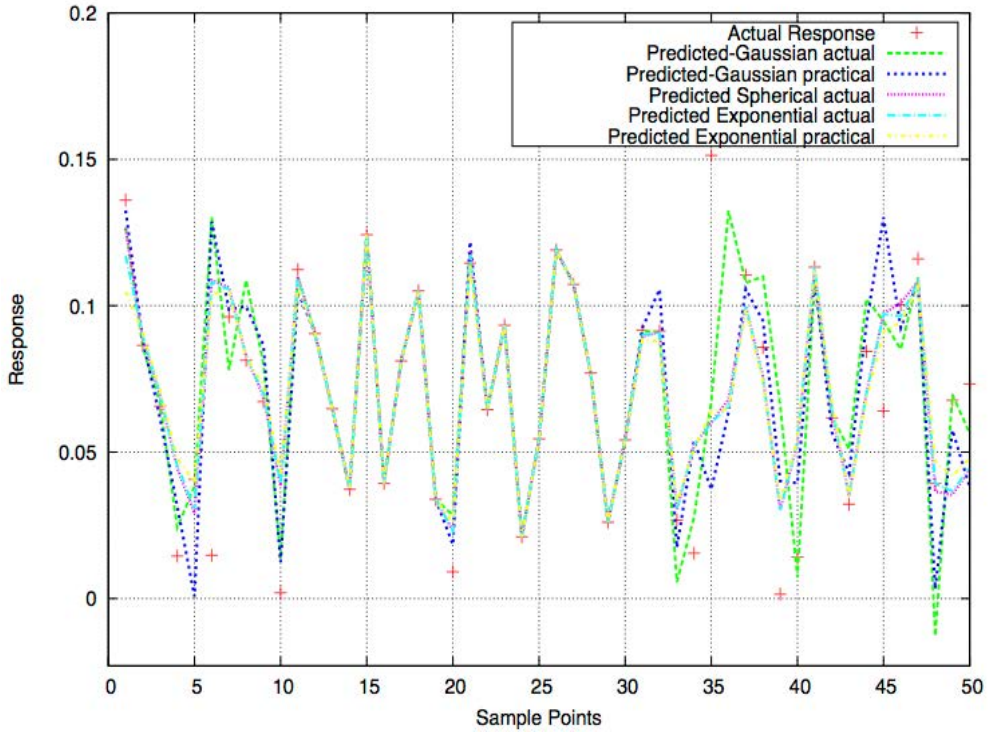

Fig. 17: Sample points and its responses (ΔCl) based on MPSOA

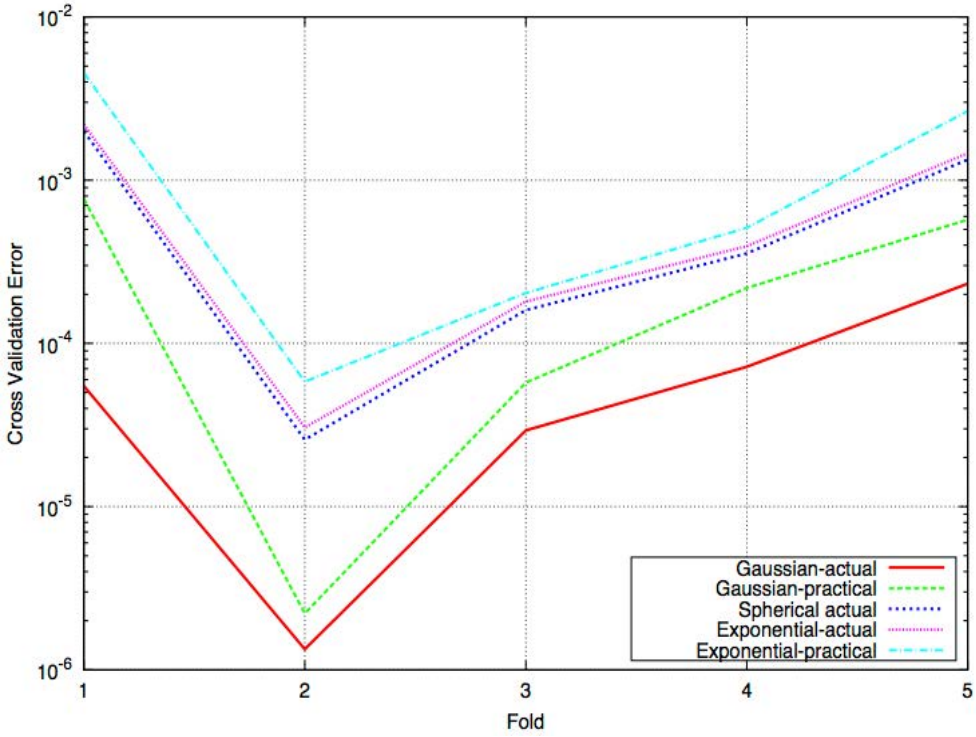

Fig. 18: CV for Low-fidelity Cl surrogate model based on PSOA

K fold cross validation: This cross validation method is used to estimate the performance of the constructed surrogate models. In this method, N sample points which are taken from PSO and MPSO algorithms are divided into k different data folds. Among the k data folds, k-1 data folds are used the train the surrogate models and the remaining one data fold is used to validate the surrogate model. The expression which is given below is used to calculate the cross validation error of the predictions. In this research, the most suitable variogram is selected based on the CV approach. The influence of different theoretical variogram models on the accuracy of the constructed surrogate model is evaluated by using the K-fold cross validation.

$$\in_{cv} = \frac{1}{(N/K)} \sum_{i=1}^{(N/K)} (\hat{F}(i) - F(i))^2 \qquad (23)$$

The comparison of cross validation error of Cl surrogate model constructed based on PSOA and MPSOA algorithms are shown in Fig. 18 and 19. In the Figures ϵ_{cv} changes in the order of 10^{-2}-10^{-6} and also it depicts that the surrogate model which is constructed by the Gaussian model with actual range is more accurate than the other models. The accuracy of the surrogate model depends on the ability of the theoretical semivariogram model in fitting with the experimental semivariogram.

The comparison of cross validation error of high fidelity Cd surrogate model constructed based on PSOA and MPSOA algorithms are shown in Fig 20 and 21. In the Figures ϵ_{cv} changes in the order of 10^{-3}-10^{-9} and also it depicts that the surrogate model which is constructed by the Exponential model with practical range is more accurate than the other models.

The comparison of cross validation error of ϵ_{cv} Cl surrogate model constructed based on PSOA and MPSOA algorithms are shown in Fig. 22 and 23. In the figures changes in the order of 10^{-3}-10^{-7} and also it depicts that the surrogate model which is constructed by the Exponential model with practical range is more accurate than the other models. Hence, based on the above analysis we have chosen the Exponential model with practical range for the construction of surrogate model.

The aerodynamic Efficiency (E) of an airfoil geometry which is placed within 'S' can be calculated using the constructed surrogate models. Once an unknown sample point (airfoil geometry and M) is generated, then it can be supplied to the three surrogate models. As discussed

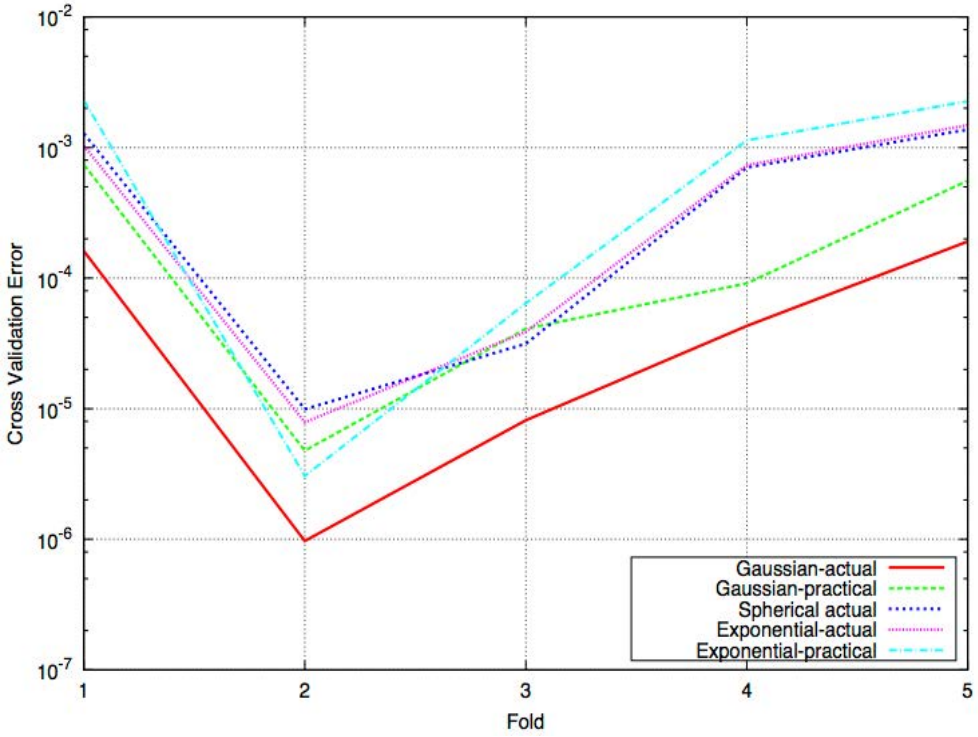

Fig. 19: CV for low-fidelity Cl surrogate model based on MPSOA

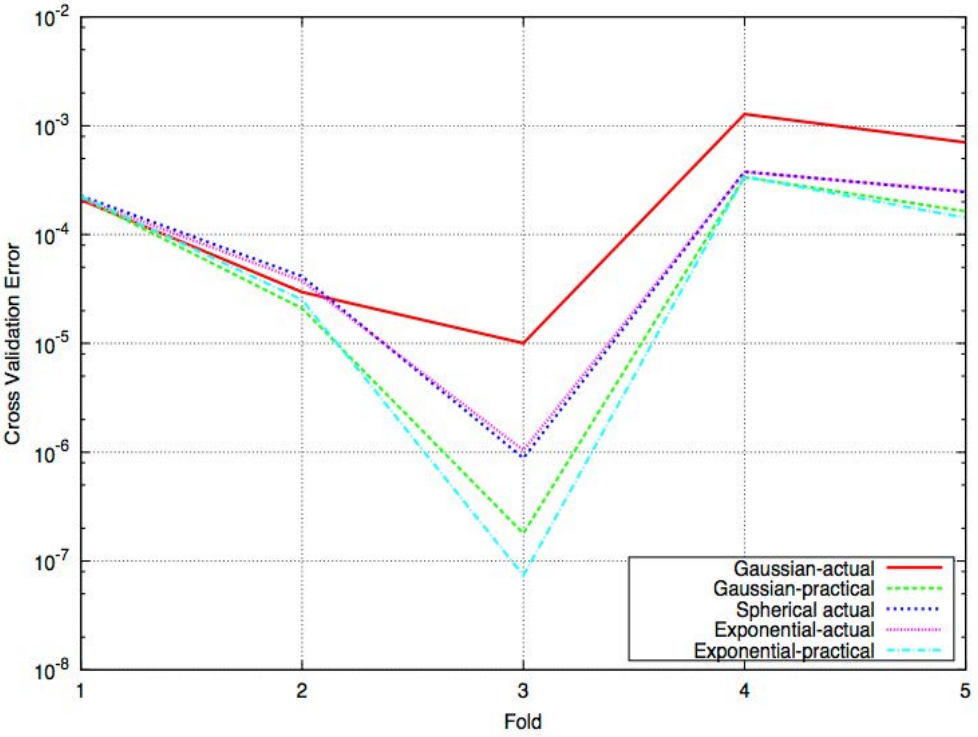

Fig. 20: CV for High-fidelity Cd surrogate model based on PSOA

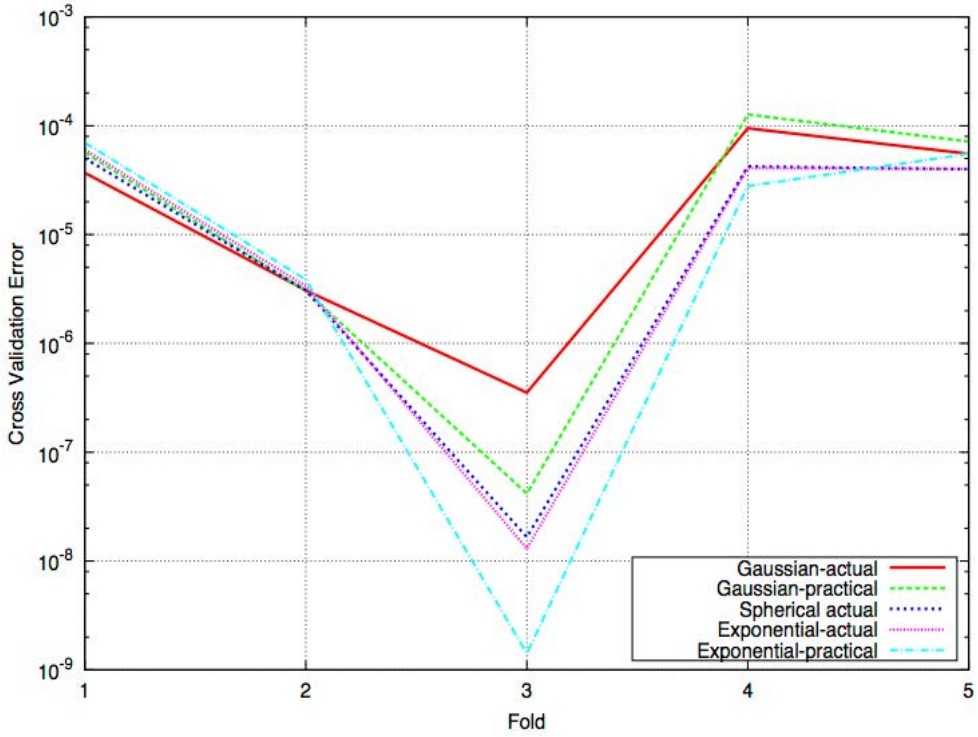

Fig. 21: CV for High-fidelity Cd surrogate model based on MPSOA

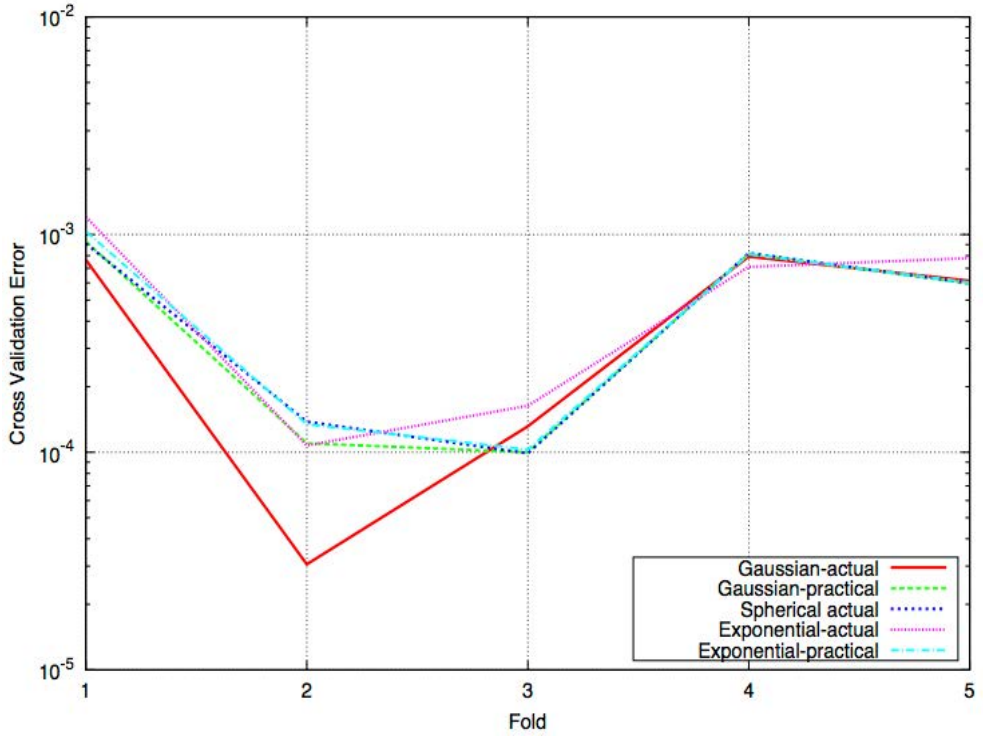

Fig. 22: CV for ΔCl surrogate model based on PSOA

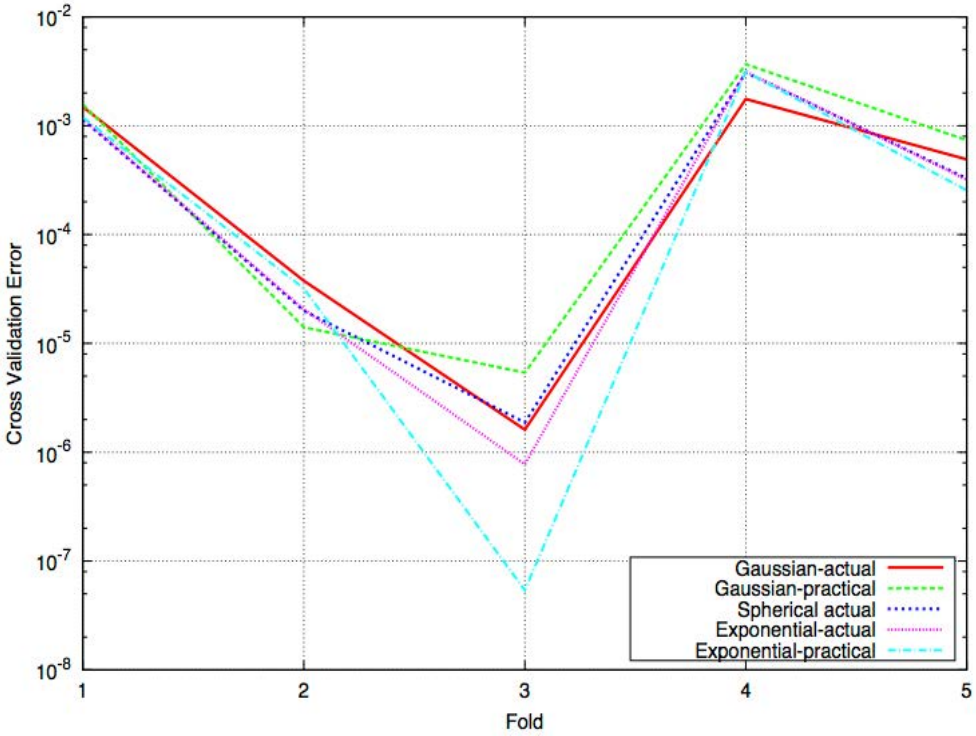

Fig. 23: CV for ΔCl Surrogate model based on MPSOA

earlier, the first surrogate model can predict the low-fidelity Cl while the second one can predict the high-fidelity C_d. The Δc_l can be predicted by the third surrogate model. Now, the E of the airfoil at α = 5.0 deg for the above discussed flow conditions can be calculated from the following relations. Since, the airfoil is placed within 'S', the M will have a value between 0.1 and 0.6:

$$(C_l)_{\text{High-fidelity}} = (C_l)_{\text{Low-fidelity}} - \Delta C_l \quad (24)$$

$$E = \frac{L}{D} = \frac{(C_l)_{\text{High-fidelity}} q_\infty S}{(C_d)_{\text{High-fidelity}} q_\infty S} \quad (25)$$

Where:

L = The lift force of the airfoil
D = The drag force of the airfoil
q = The dynamic pressure of the flow
p = The density of the flow
V = The velocity of the flow and
S = The surface area of the airfoil

Since, S and q are constant for a given airfoil and flow conditions (M p, Temperature), respectively, the above relation can be written as follows:

$$E = \frac{L}{D} = \frac{(C_l)_{\text{High-fidelity}}}{(C_d)_{\text{High-fidelity}}} \quad (26)$$

In order to validate the proposed strategy, the E is estimated at various sample points (i.e., airfoil geometries) placed within the design space 'S' using the constructed surrogate models. The estimated values are compared with the actual values of E which are calculated from separate CFD simulations.

The constructed surrogate models have been coupled with the PSO and MPSOA algorithm with parameters for controlling the ASO being summarised at Table 2. The ASO process is carried out for maximum E. An optimised solution which has an aerodynamic efficiency of E = 87.376 is obtained through MPSO algorithm and the PSO algorithm produces an aerodynamic efficiency of E = 85.13. The flow around the optimised airfoil geometry which is generated by the MPSO algorithm is solved in FLUENT using the corresponding flow properties as shown in Table 3. The CFD calculations show that the optimised airfoil geometry has E = 84.641 corresponding to a 2.74% error. The obtained airfoil geometry is still better than the baseline shape which has 68.091 for the flow conditions tabulated in Table 4. It can then be confirmed that the optimised geometry has 19.285% of improvement in E over the actual NACA 2411 at the specified flow conditions.

Table 3: Flow properties to solve the optimised geometry

Property	Value
Pressure (p)	101325 N m^{-2}
Density (p)	1.1766 kg m^{-3}
Temperature (T)	300 K
Mach (M)	0.331351
Velocity (V)	115.05
Re	7.337×10^{6}
I	0.022%
μ	1.845×10^{-5} k g^{-1} sec

CONCLUSION

A new statistical strategy is proposed to construct surrogate models for actual CFD algorithms in order to get high-fidelity predictions of aerodynamic forces (C_l, C_d) and aerodynamic Efficiency (E) from the commodiously available low fidelity data and limited high-fidelity data. An ASO problem is formulated and solved using PSO and Modified PSO algorithm. The constructed surrogate models are used in the place of actual CFD algorithms during the optimisation. If an actual CFD algorithm is employed for solving the flow during the optimisation, several days would have been required for obtaining the optimised solution. This is due to the time taken for a single CFD simulation during the data mining process. It can be clearly observed that the proposed strategy has drastically reduced the required computational time and resources to carry out an ASO problem. It is observed that the method of parameterisation scheme is crucial for both surrogate model construction and optimiser since its variables are used as the design and optimisation variables. PARSEC parameterisation scheme is provides effectiveness since it offers flexibility in controlling the aerodynamic characteristics of the airfoil geometry with a minimum number of parameters. The statistically unbiased characteristics of the Ordinary Kriging approach enhance the ability and accuracy of the surrogate models in predicting response values at an unexplored space. MPSO algorithm is observed to be more effective in exploring the search space when compared to the PSO algorithm. Since the variability exists in all the generations of the MPSO, huge numbers of desirable solutions to the defined problem are generated. Hence this process can also be considered as a data mining process and can be further used for airfoil design and analysis.

REFERENCES

Alexander, K. and E. Tadmor, 2010. New high-resolution central schemes for nonlinear conservation laws and convection-diffusion equations. J. Comput. Phys., 160: 214-282.

Balu, R. and U. Selvakumar, 2009. Optimum hierarchical Bezier parameterization of arbitrary curves and surfaces. Proceeding of the 11th Annual CFD Symposium, August, 2009, Indian Institute of Science, Bangalore, India, pp: 46-48.

Balu, R., S. Ulaganathan and N. Asproulis, 2012. Effect of variogram types on surrogate model based optimisation of aircraft wing shapes. Procedia Eng., 38: 2713-2725.

Castonguay, P. and S.K. Nadarajah, 2007. Effect of shape parameterization on aerodynamic shape optimization. Proceedings of the 45th AIAA Conference on Aerospace Sciences Meeting and Exhibit, January 8-11, 2007, AIAA, Reno, Nevada, pp: 1-20.

Deepa, S.N. and G. Sugumaran, 2011. MPSO based model order formulation technique for SISO continuous systems. J. Eng. Appl. Sci., 7: 125-130.

Deepa, S.N. and G. Sugumaran, 2012. New results on discrete PID controller design by MPSO based lower order model. J. Elect. Control Eng., 2: 22-28.

Duchaine, F., M.T. Morel and L.Y. Gicquel, 2009. Computational-fluid-dynamics-based kriging optimization tool for aeronautical combustion chambers. AIAA. J., 47: 631-645.

Giunta, A.A., 1997. Aircraft multidisciplinary design optimization using design of experiments theory and response surface modeling methods. MSc Thesis, Virginia Tech University, Blacksburg, Virginia.

Hess, J.L., 1990. Panel methods in computational fluid dynamics. Ann. Rev. Fluid Mech., 22: 255-274.

Jouhaud, J.C., P. Sagaut, M. Montagnac and J. Laurenceau, 2007. A surrogate-model based multidisciplinary shape optimization method with application to a 2D subsonic airfoil. Comput. Fluids, 36: 520-529.

Katz, J. and A. Plotkin, 1991. Low-Speed Aerodynamics from Wing Theory to Panel Methods. 2nd Edn., McGraw-Hill, Inc., New York.

Khurana, M.S., H. Winarto and A.K. Sinha, 2009. Airfoil optimization by swarm algorithm with mutation and artificial neural networks. AIAA Aerospace Sciences Meeting Including The New Horizons Forum and Aerospace Exposition, 2009.

Liang, Y., X.Q. Cheng, Z.N. Li and J.W. Xiang, 2011. Robust multi-objective wing design optimization via CFD approximation model. Eng. Appl. Comput. Fluid Mech., 5: 286-300.

Mukesh, R., K. Lingadurai and U. Selvakumar, 2014. Kriging methodology for surrogate-based airfoil shape optimization. Arabian J. Sci. Eng., 39: 7363-7373.

Mukesh, R., R. Pandiyarajan, S. Ulaganathan and K. Lingadurai, 2012. Influence of search algorithms on aerodynamic design optimization of aircraft wings. Int. J. Soft Comput., 7: 79-84.

Ping, X.U. and C. Jiang, 2008. Aerodynamic optimization design of airfoil based on particle swarm optimization. Aircraft Design, 28: 6-9.

Qin, M.A., D.C. Xin and X.H. Wang, 2009. A modified particle swarm optimization algorithm. Natural Sci., 1: 151-155.

Raymer, D., 2002. Enhancing aircraft conceptual design using multidisciplinary optimization. MSc Thesis, Royal Institute of Technology, Stockholm, Sweden.

Rodriguez, J.D., A. Perez and J.A. Lozano, 2010. Sensitivity analysis of k-fold cross validation in prediction error estimation. IEEE. Trans. Pattern Anal. Mach. Int., 32: 569-575.

Sacks, J., W.J. Welch, T.J. Mitchell and H.P. Wynn, 1989. Design and analysis of computer experiments. Stat. Sci., 4: 409-423.

Sheldahl, R.E. and P.C. Klimas, 1981. Aerodynamic Characteristics of Seven Airfoil Sections Through 180 Degrees Angle of Attack for Use in Aerodynamic Analysis of Vertical Axis Wind Turbines. Sandia National laboratories, Albuquerque, New Mexico.

Sobieczky, H., 1998. Parametric airfoils and wings. Notes Num. Fluid Mech., 68: 71-88.

Spalart, P.R. and S.R. Allmaras, 1992. A one-equation turbulence model for aerodynamic flows. Proceedings of the 30th Aerospace Sciences Meeting and Exhibit, Reno, NV. USA., Jan. 6-9, American Institute of Aeronautics and Astronautics, pp: 1-23.

Stein, M.L., 1999. Interpolation of Spatial Data: Some Theory for Kriging. Springer Verlag, Germany, ISBN: 9780387986296, Pages: 247.

Ulaganathan, S., I. Couckuyt, T. Dhaene, J. Degroote and E. Laermans, 2016. Performance study of gradient-enhanced Kriging. Eng. Comput., 32: 15-34.

Wilcox, D.C., 1993. Turbulence modelling for CFD. DCW Industries Inc, Canada, California.

Yang, W.S., C.H. Kung and C.M. Kung, 2011. Image Enhancement Using the Multi-Scale Filter: Application of the Bilateral Filtering Scheme and PSO Algorithm. In: Theoretical and Mathematical Foundations of Computer Science, Zhou, Q. (Ed.). Springer, Berlin, Germany, ISBN:978-3-642-24998-3, pp: 508-514.

Zang, T.A. and L.L. Green, 1999. Multidisciplinary design optimization techniques: Implications and opportunities for fluid dynamics research. Proceedings of the 30th AIAA Conference on Fluid Dynamics, Jun 28- July 1, 1999, AIAA, Norfolk, Virginia, pp: 1-21.